

White light supercontinuum generation in a Y-shaped microstructured tapered fiber pumped at 1064 nm

J. Cascante-Vindas, A. Díez,* J. L. Cruz, and M.V. Andrés

Universidad de Valencia, Departamento de Física Aplicada-ICMUV, Dr. Moliner 50, 46100 Burjassot, Spain

*antonio.diez@uv.es

Abstract: We report the generation of supercontinuum in a Ge-doped Y-shape tapered fiber pumped at 1064 nm in the ns pump regime. The taper was designed to have long taper transitions and a taper waist with a core diameter of 0.9 μm . The large air-filling fraction and diameter of the air-hole microstructure reduces the confinement loss at long wavelengths so, enabling the extension of the spectrum to longer wavelengths. Along the taper transition the zero-dispersion wavelength decreases as the diameter of the taper becomes smaller. The spectral components generated along the taper transition pump the taper waist, enhancing the generation of short wavelengths. A flat spectrum spanning from 420 nm to 1850 nm is reported.

©2010 Optical Society of America

OCIS codes: (060.4005) Microstructured fibers; (060.4370) Nonlinear optics, fibers; (230.2285) Fiber devices and optical amplifiers.

References and links

1. J. K. Ranka, R. S. Windeler, and A. J. Stentz, "Visible continuum generation in air-silica microstructure optical fibers with anomalous dispersion at 800 nm," *Opt. Lett.* **25**(1), 25–27 (2000).
2. J. M. Dudley, G. Genty, and S. Coen, "Supercontinuum generation in photonic crystal fiber," *Rev. Mod. Phys.* **78**(4), 1135–1184 (2006).
3. A. Ferrando, E. Silvestre, P. Andrés, J. J. Miret, and M. V. Andrés, "Designing the properties of dispersion-flattened photonic crystal fibers," *Opt. Express* **9**(13), 687–697 (2001).
4. G. Renversez, B. Kuhlmeiy, and R. McPhedran, "Dispersion management with microstructured optical fibers: ultraflattened chromatic dispersion with low losses," *Opt. Lett.* **28**(12), 989–991 (2003).
5. S. G. Leon-Saval, T. A. Birks, W. J. Wadsworth, P. St. J. Russell, and M. W. Mason, "Supercontinuum generation in submicron fibre waveguides," *Opt. Express* **12**(13), 2864–2869 (2004).
6. J. Cascante-Vindas, A. Díez, J. L. Cruz, M. V. Andrés, E. Silvestre, J. J. Miret, and A. Ortigosa-Blanch, "Tapering photonic crystal fibres for supercontinuum generation with nanosecond pulses at 532 nm," *Opt. Commun.* **281**(3), 433–438 (2008).
7. J. Teipel, D. Türke, H. Giessen, A. Zintl, and B. Braun, "Compact multi-Watt picosecond coherent white light sources using multiple-taper fibers," *Opt. Express* **13**(5), 1734–1742 (2005).
8. J. C. Travers, S. V. Popov, and J. R. Taylor, "Extended blue supercontinuum generation in cascaded holey fibers," *Opt. Lett.* **30**(23), 3132–3134 (2005).
9. C. M. B. Cordeiro, W. J. Wadsworth, T. A. Birks, and P. St. J. Russell, "Engineering the dispersion of tapered fibers for supercontinuum generation with a 1064 nm pump laser," *Opt. Lett.* **30**(15), 1980–1982 (2005).
10. F. Lu, Y. Deng, and W. H. Knox, "Generation of broadband femtosecond visible pulses in dispersion-micromanaged holey fibers," *Opt. Lett.* **30**(12), 1566–1568 (2005).
11. A. Kudlinski, A. K. George, J. C. Knight, J. C. Travers, A. B. Rulkov, S. V. Popov, and J. R. Taylor, "Zero-dispersion wavelength decreasing photonic crystal fibers for ultraviolet-extended supercontinuum generation," *Opt. Express* **14**(12), 5715–5722 (2006).
12. J. M. Stone, and J. C. Knight, "Visibly 'white' light generation in uniform photonic crystal fiber using a microchip laser," *Opt. Express* **16**(4), 2670–2675 (2008).
13. J. Cascante-Vindas, S. Torres-Peiró, A. Díez, and M. V. Andrés, "Supercontinuum generation in highly Ge-doped core Y-shaped microstructured optical fiber," *Appl. Phys. B* **98**(2-3), 371–376 (2010).
14. T. Boris, "Confinement loss in adiabatic photonic crystal fiber tapers," *J. Opt. Soc. Am. B* **23**, 1965–1974 (2006).
15. S. Torres-Peiró, A. Díez, J. L. Cruz, and M. V. Andrés, "Fundamental-mode cutoff in liquid-filled Y-shaped microstructured fibers with Ge-doped core," *Opt. Lett.* **33**(22), 2578–2580 (2008).
16. W. Wadsworth, A. Witkowska, S. Leon-Saval, and T. A. Birks, "Hole inflation and tapering of stock photonic crystal fibres," *Opt. Express* **13**(17), 6541–6549 (2005).
17. A. Hochman, and Y. Leviatan, "Efficient and spurious-free integral-equation-based optical waveguide mode solver," *Opt. Express* **15**(22), 14431–14453 (2007).

1. Introduction

In the last years, the generation of supercontinuum (SC) and dispersion engineering have been a subject of strong interest [1–4] since the advent of microstructured fibers (MFs). Many efforts have been done to achieve efficient generation in the blue and UV wavelength range. The generation of short wavelengths requires a fiber with a zero-dispersion-wavelength (ZDW) close to the visible and a pump source emitting close to the ZDW. A basic scheme consists on the use of a doubled-frequency Nd:YAG laser emitting at 532 nm and a small-core MF. Microchip passively Q-switched Nd:YAG lasers emitting sub-ns pump pulses meet the requirements for SC generation and are low-cost and compact sources. The core diameter of the MF must be $< 1 \mu\text{m}$ in order to shift the ZDW close to 532 nm. Consequently, the pump coupling into the MF is highly critical and unstable. Alternatively, it has been reported the use of conventional fiber tapers or tapers fabricated from MFs [5,6], in which the light is focused into the large core of the untapered fiber. The taper transition couples adiabatically the light into the small core. However, high energy ns pulses at 532 nm easily damage the core of the thin fiber taper, which limits the extension of the SC and the power spectral density.

Several approaches for visible light generation using inexpensive lasers emitting around 1064 nm have been reported. Some of them are based on multi-stage arrangements with decreasing ZDW [7–9]. In a basic scheme, a fiber or taper with ZDW close to 1064 nm is used to generate spectral components at short wavelengths. Those short-wavelength components pump a second fiber/taper, the ZDW of which is closer to the visible range. Based on a similar idea it has been reported the generation of SC in several continuously-decreasing ZDW fiber components. In [10], SC spectra extending from 400 nm to 1200 nm was generated in a short fiber taper transition (10 mm long) pumped in the fs regime. In [11], a few meters long tapered MF fabricated in a fiber drawing tower was pumped with a ns pump laser (9 kW peak power), generating an SC spectra from 370 nm to beyond 1750 nm. Alternatively, efficient generation of visible and UV light using a 1064 nm pump source was also demonstrated using an MF with conveniently designed dispersion and group index [12].

In a previous work, we reported experimental results on the generation of SC in a Ge-doped core Y-shaped microstructured fiber [13]. In those experiments, the fiber was pumped using a microchip laser emitting 600 ps duration pulses at 1064 nm. A flat SC spectra spanning from 550 nm to beyond 1750 nm was generated in 5 m of fiber. The extension of the SC towards the visible and UV was constrained by the characteristics of dispersion and group index of the fiber. Here, we report experimental results on SC generation in a taper fabricated from the Ge-doped Y-shape fiber mentioned above. The taper was made with long transitions. The first ZDW of the taper waist was shifted down to 647 nm. Because of the long transitions, this single taper behaves as a two-stage arrangement, where the ZDW decreasing transition generates spectral components near the first ZDW of the taper waist, which subsequently extends the spectrum towards even shorter wavelengths. With similar pump conditions than in [13], a SC spectrum spanning from 420 nm to 1850 nm was generated. To our acknowledgment, it is the widest SC generated in a single microstructured fiber taper in the ns pump regime using a 1064 nm pump source.

By tapering the MF the interaction length required for SC generation can be reduced from several meters to some tens of centimeters. As an example, in [12] the short wavelength edge of the SC was extended down to 400 nm using a 10 m long MF, while the length of the taper used for the results reported here was ~ 35 cm long. In addition, the core diameter at the taper waist is submicrometric, thus the fields overlap strongly with the holes. This special feature, in conjunction with the capability of the taper to generate the SC, could eventually be exploited for the design of monolithic and compact gas sensors or gas cells where the taper generates the broadband light source and also allows strong light interaction with the gas filling the holes.

Owing to the large air holes of the Y-shape fiber, the fabrication of the taper did not require tight control of the pressure within the holes during the taper fabrication. In addition, the large diameter of the microstructure, as well as the large air-filling fraction in the taper keeps low the confinement loss at long wavelengths [14].

The Ge doping of the core increases the nonlinear refractive index [9] and the Raman gain [10], and it reduces the modal effective area, thus enhancing nonlinear effects. Additionally, it allows, if necessary, collapsing the air holes while maintaining guidance, and it facilitates low-loss splicing to standard single mode fibers.

2. Fabrication

The fiber used for the fabrication of the tapers is shown in Fig. 1 (a). It is a solid-core MOF with Y-shaped cross section and three large air holes in the cladding. Three narrow and long bridges sustain the core at the centre of the fiber. The diameter of the core was $\sim 5.5 \mu\text{m}$. The central region of the core of about $6.5 \mu\text{m}^2$ area was Ge-doped ($\text{NA} = 0.29$). The diameter of the air-hole microstructure was $65 \mu\text{m}$ and the outer diameter of the fiber was $102 \mu\text{m}$. The fiber is few-moded at visible wavelengths. More details about the fabrication and the guiding characteristics of this fiber can be found in [13,15].

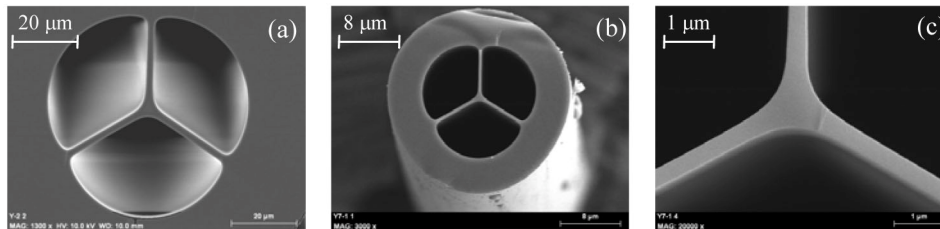


Fig. 1. SEM images of (a) the fiber used to fabricate the tapers, and (b)-(c) the taper.

The fiber was tapered using a traveling-flame elongation method. The flame temperature was controlled by adjusting the gas mixture (butane/oxygen). In general, when tapering an MF, surface tension causes collapse of the air holes as the fiber is heated. As a consequence, the air-filling fraction decreases, the effective area increases, and the nonlinear parameter, γ , becomes smaller. Additionally, the confinement loss at long wavelengths increases [14]. The technique that is mostly followed to counteract the air hole collapse consists on applying a pressure of an inert gas into the holes while the fiber is being tapered [6,16]. The pressure required depends inversely on the diameter of the holes [16]. Typical pressure values for tapering conventional PCFs are about 6-7 bar. One advantage of using the Y-shaped fiber (with very large air holes) for tapering is that lower pressure values are required.

Following the method described above, several Y-shaped microstructured fiber tapers were made. The resulting tapers had a 130 mm long uniform waist of $25 \mu\text{m}$ outer diameter, with 110 mm long transitions. The core diameter at the taper waist was $0.9 \mu\text{m}$. SEM images of one of the fabricated tapers, which was used for the SC generation experiments, are shown in Fig. 1 (b)-(c). An excess pressure of just 0.5 bar in the holes was enough to preserve the very large air filling fraction of the original fiber in the taper. We also fabricated tapers without pressurizing the holes and, although the hole collapse was small, we did observe that those tapers showed slightly higher transmission losses at long wavelengths.

3. Experimental results

We used a compact Q-switched Nd:YAG microchip laser emitting at 1064 nm (0.6 ns duration pulses, 20 kHz repetition rate) as the pump source for the SC generation experiments. The maximum average output power of the laser is 160 mW, corresponding to a peak power of 13 kW, approximately. The pump was launched into the fiber taper at the beginning of the transition, where the dimensions are those of the initial fiber, which allows achieving a large pump coupling efficiency. A $\times 16$ aspheric lens was used to focus the beam into the core.

Figure 2 shows some SC spectra recorded at different pump power levels. The spectral resolution was 5 nm. At low pump power, three bands can be observed along with the pump signal. These bands are centered at 1053 nm, 1075 nm and 1113 nm. As the pump power was increased, the intensity of the bands increased and, at 1.4 kW of peak power, the spectral broadening is already considerable. As the pump power level was increased further, the spectrum exhibits a continuous broadening towards both sides of the pump wavelength. At the highest pump power, 3.2 kW peak power, the spectrum spans over more than 1400 nm, from 420 nm to 1850 nm. The spectrum generated at the highest pump power is remarkably flat; from 850 nm to 1500 nm the intensity variation is within 3 dB. The long wavelength side of the spectrum was measured with an OSA Yokogawa AQ6375, which has no order-sorting filters. Thus, a 1.3 μm cut-on long pass filter was used to prevent multi-order interference in the measurement.

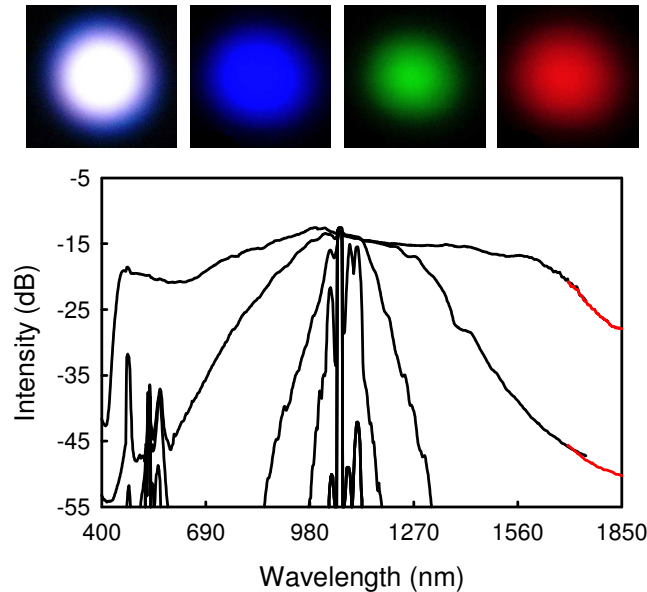


Fig. 2. (top) Far-field pattern of the output beam unfiltered (left), and filtered with different visible bandpass filters. (bottom) SC output spectrum for different pump power levels. The pulse peak powers were 0.9 kW, 1.1 kW, 1.4 kW, 1.8 kW, 3.2 kW. Black and red traces were measured with different optical spectrum analyzers (ANDO AQ6315A and Yokogawa AQ6375, respectively).

At the highest pump power level, the output from the tapered fiber was essentially white. The continuum was observed to be generated in the fundamental mode. Figure 2 shows some images of the output far-field pattern unfiltered or passed through visible bandpass filters, where no evidences of higher order modes can be observed.

A further 10% increase in pump power (up to 3.5 kW peak power, approximately) caused the damage of the taper at the end of the taper waist. Figure 3 (a) shows a photograph of the taper taken when this happened. The visible components of the scattered light are very similar to those observed previously at the taper's output. The pump power level was kept constant and, after few minutes, the taper resulted damaged again but now at the end of the first transition, i.e. at the beginning of the uniform waist. A photograph of the taper when this happened is shown in Fig. 3 (a). The scattered light at this point contains red spectral components, which indicates that a significant contribution to the resulting SC spectrum is generated in the taper transition. Another important consequence of the spectral broadening at the input transition is that the signal entering the taper waist, which acts as the pump for the nonlinear effects in this taper section, is spectrally very broad and it does not only contain the 1064 nm signal from the pump laser. To confirm that the long transitions contribute

significantly to spectral broadening, a second taper with similar structure was fabricated. Figure 3 (b) shows the spectrum of emerging light from (i) the output of the taper, (ii) the end of the input taper transition, and (iii) the start of the taper transition. Although the pump power was lower than in the previous experiment, a broad spectrum was recorded at the end of the input transition.

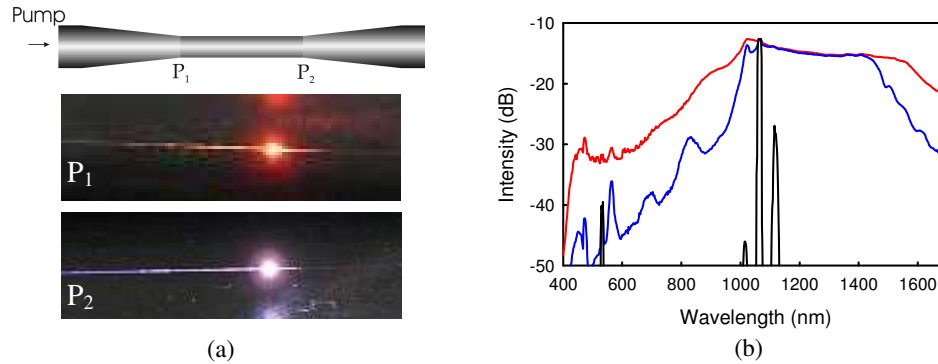


Fig. 3. (a) Schematic of the taper indicating the damaged points. Photograph of the light scattered when the first taper was damaged at P₁ and at P₂. (b) SC generation in a second taper. Spectrum of light emerging from the taper's output (red), at the end of the input transition (blue), and at the beginning of the input transition (black). Pulse peak power: 2.4 kW.

4. Discussion

Theoretical calculations of the basic guiding properties were carried out using a source-model technique [17]. This approach allows modeling fibers with arbitrary refractive-index distributions, thus, the real refractive index profile was taken into account. Figure 4(a) shows the dispersion of the fundamental mode propagating in the taper waist, and in the untapered fiber. In the case of the untapered fiber, the first ZDW is 1195 nm, while the second ZDW is out of the calculation range. As the scale of the fiber is reduced, both first and second ZDW shift to shorter wavelengths. The dispersion of the taper waist shows two zero dispersion wavelengths centered at 647 nm and 1127 nm, being the dispersion anomalous at the wavelength range between the two ZDWs. Figure 4 (b) shows the evolution of the first ZDW along the taper transition. The dispersion at the pump wavelength is anomalous in most of the transition length, with the exception of the first few mm.

From the experimental SC spectra (see Fig. 2), we can infer that the process of SC generation is initiated by MI, as it is shown at low pump power, where a pair of symmetrically-located peaks appears on both sides of the pump. A third band located at 1113 nm corresponds to stimulated Raman scattering (SRS) generated by the pump, probably, along the section of the taper with normal dispersion. Notice that the generation of SRS is enhanced by the presence of GeO₂ in the fiber [18].

The spectral broadening in the taper can be understood as a two-stage process, i.e., generation along the input taper transition, and along the taper waist. We believe that the mechanism involved in the spectral broadening along the taper transition is analogous to what it was reported in [11], since the experimental conditions are quite similar, except for the length scale. The ZDW decreasing along the transition allows the four-wave mixing (FWM) phase-matching condition to be satisfied for a wide range of wavelengths. A cascaded FWM process along the taper transition is enabled, which would extend the spectrum on either side of the pump wavelength. At a given point of the transition, the spectral components generated in the normal dispersion regime allow shorter wavelengths to be generated via FWM in the next section of the transition. In particular, the extension towards the visible reaches the red wavelengths as shown in Fig. 3(a). Simultaneously, Raman self-frequency shifted solitons

(SSFS) propagating in the taper transition will contribute to the generation towards longer wavelengths.

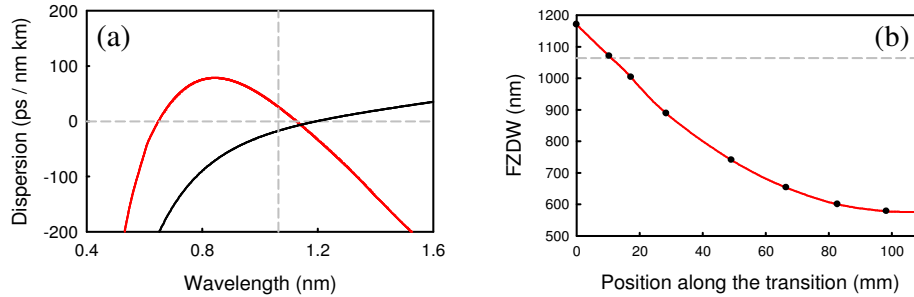


Fig. 4. (a) Dispersion as a function of wavelength of the fundamental mode of the untapered fiber (black) and the taper waist (red). (b) Evolution of the first ZDW along the taper transition. Dashed line indicates the pump wavelength.

The broadband light generated in the taper transition pumps the uniform taper waist. The dispersion in the taper waist for many of the spectral components generated in the transition is anomalous, i.e. those laying between the two ZDWs. As shown in Fig. 3(a), at high pump power levels the taper transition generates red components, which are close to the first ZDW of the taper waist. It is also expected that the beam entering the taper waist would contain components close to its second ZDW. Therefore, a multi-FWM process is enabled in the taper waist, which extends the spectrum towards even shorter wavelengths, as it has been observed previously in multiple tapers configurations [9]. We believe that the contribution to the spectral broadening of SSFS generated by the pump in the taper waist is small, since the wavelength range where solitons can be generated, i.e. between the pump and the second ZDW, is quite narrow.

7. Conclusion

We have reported experimental results on the SC generation in a taper fabricated from a Ge-doped Y-shape fiber. The taper was pumped at 1064 nm wavelength in the ns pump regime using a Q-switched microchip laser. The taper can be understood as a multi-stage configuration formed by the taper transitions where the ZDW changes continuously and the taper waist. The two ZDWs in the taper waist were 647 nm and 1127 nm. The spectral components generated along the input taper transition pump the taper waist, the dispersion of which is anomalous for many of them. Therefore, a multi-FWM process is enabled in the taper waist. At a pump pulse peak power of 3.2 kW, a broad spectrum is reported. The spectrum extends from 420 nm to 1870 nm when measured at -20 dB, and from 850 nm to 1500 nm when measured at -3 dB.

Acknowledgements

This work has been financially supported by the Ministerio de Educación y Ciencia and the Generalitat Valenciana of Spain (projects TEC2008-05490 and PROMETEO/2009/077, respectively).